ARTICLES: Investigative Ophthalmology & Visual Science

Mycoplasma ocular infection in subretinal graft transplantation of iPS cells-derived retinal pigment epithelial cells

Running title: Mycoplasma infection in iPS-RPE transplantation

Kenichi Makabe,[1,2] Sunao Sugita,[1] Ayumi Hono,[1] Hiroyuki Kamao[3] & Masayo Takahashi[1]

[1]Laboratory for Retinal Regeneration, Center for Biosystems Dynamics Research, RIKEN, 2-2-3 Minatojima-minamimachi, Chuo-ku, Kobe 650-0047, Japan; [2]Kyoto University Graduate School of Medicine, Yoshidakonoe-cho, Sakyo-ku, Kyoto 606-8501, Japan; [3]Department of Ophthalmology, Kawasaki Medical School, 577 Matsushima, Kurashiki, Okayama 701-0192, Japan.

Corresponding author: Sunao Sugita, Laboratory for Retinal Regeneration, Center for Biosystems Dynamics Research, RIKEN, 2-2-3 Minatojima-minamimachi, Chuo-ku, Kobe 650-0047, Japan. Tel: +81-78-306-3305; Fax: +81-78-306-3303; E-mail: sunaoph@cdb.riken.jp

Abstract

Purpose: To report occurrence of acute severe inflammation after surgical implantation of mycoplasma infected iPS cells-derived retinal pigment epithelial (iPS-RPE) cells into the eyes of healthy primates, and determine the immunopathological mechanisms of the inflammation.

Methods: Ophthalmic allogeneic transplantation of iPS-RPE cells was performed in the subretina of major histocompatibility complex (MHC)-matched (two eyes) and MHC-mismatched (one eye) healthy cynomolgus monkeys. The clinical course after transplantation was observed using color fundus photography, fluorescence angiography, and optical coherence tomography. After the animals were sacrificed at one month after surgery, eyeballs were removed and pathologically examined. Microorganisms were analyzed by PCR methods and BLAST analysis using preserved graft iPS-RPE cells and the recipients' vitreous humor. Mixed lymphocyte-RPE assay was performed on the mycoplasma-infected and non-infected iPS-RPE cells *in vitro*.

Results: In tested eyes, abnormal findings were observed in the grafted retina two weeks post-surgery. Here, we observed retinal vasculitis and hemorrhage, retinal detachment, and infiltration of inflammatory cells into the retina of the eyes. One month post-surgery, animals were sacrificed due to the severe immune responses observed. Using PCR methods, sequence analysis detected mycoplasma DNA (*Mycoplasma arginini* species) in both the grafted RPE cells and the collected vitreous fluids of the monkeys. Mixed lymphocyte-RPE assay revealed that the infected iPS-RPE cells enhanced the proliferation of inflammatory cells *in vitro*.

Conclusions: Transplantation of graft iPS-RPE cells contaminated with mycoplasma into the subretina caused severe ocular inflammation. Mycoplasma possesses the ability

to cause immune responses in the host.

(Word count: 244)

Keywords: Mycoplasma, Ocular inflammation, Transplantation, iPS cells, Retinal pigment epithelial cells, Regenerative medicine.

Introduction

Recent developments in the field of regenerative medicine have made it possible to transplant cultured cells into patients for the treatment of diseases such as retinal disorders. However, in order to achieve a successful transplantation, it is necessary to be able to detect the presence of infectious agents. In a previous study, we reported on examination methods that can be used to study postoperative endophthalmitis caused by bacteria species [1]. However, infectious endophthalmitis caused by microorganisms other than bacteria or fungal species has yet to be examined in detail. It has also been previously reported that ocular inflammation, such as endophthalmitis and uveitis, occurs in a rodent model in which mycoplasma is directly administered into the eye [2, 3]. These mycoplasma animal models were shown to exhibit severe immune responses in the eye. On the other hand, ocular inflammation associated with *Mycoplasma pneumoniae* (*M. pneumoniae*) infections in humans has been reported [4-6]. In several other cases, mycoplasmas have been suggested to have the ability to cause ocular inflammation. One of the remarkable infection routes reported for mycoplasma involves transplantation surgery in which mycoplasma from a donor ends up causing an infection in the transplant recipient. In fact, there have been reports documenting the transfer of mycoplasma from the donor via a transplanted heart or lung [7, 8] and blood vessels [9] that ultimately caused pleurisy, surgical site infection and sepsis. Moreover, it is also possible that cultured cells can often be infected with mycoplasma. Another study reported that mycoplasma infection altered the gene expression of many inflammatory cytokines [10]. However, as far as we know, there have yet to be any reports that have shown that mycoplasma can cause severe ocular inflammation by directly invading the eye during intraocular surgery.

In the present study, we detected mycoplasma in cases of severe ocular inflammation that occurred after iPS-RPE cell transplant surgery in the vitreous of the recipient and in the stock of the grafted iPS cells-derived retinal pigment epithelial

(iPS-RPE) cells used in the transplant. In order to verify the presence of mycoplasma in the eye, we conducted the following evaluations: *(1)* Detection of the mycoplasma genome by performing molecular biological analysis using vitreous fluids and transplanted RPE cells, *(2)* Performing detailed clinical and pathological examinations of inflamed eyes in order to elucidate the pattern of inflammation. In addition, in order to elucidate the immune responses of the inflammatory cells against mycoplasma, we also performed the mixed lymphocyte-RPE assay using iPS-RPE cells infected with mycoplasma and recipient blood cells.

Materials & Methods

Preparation of monkey iPS-RPE cells

We prepared iPS cells (iPSCs) from normal cynomolgus monkeys (*Macaca fascicularis*), 1121A1 iPSCs from the HT-1 MHC homozygote monkey, and 46a iPSCs from the Cyn46 MHC heterozygote monkey[11]. The monkey iPS-RPE cells were established from the iPSCs as has been previously described[11]. All of the animal experiments were approved by the RIKEN BDR Animal Experiment Committee. The care and maintenance of the monkeys conformed to the ARVO Statement for the Use of Animals in Ophthalmic and Vision Research, and the Use of Laboratory Animals, as well as to the Guidelines of the RIKEN BDR Animal Experiment Committee.

Transplantation of iPS-RPE cells into the subretinal space of monkeys

MHC-controlled monkeys (DrpZ11 and 12: adult cynomolgus monkeys: Ina Research) and a normal control cynomolgus monkey (TLHM-6) were used in this study. For transplantation of the iPS-RPE cell suspension (MHC homozygote 1121A1 iPS-RPE cells or MHC heterozygote 46a iPS-RPE cells), we injected the subretinal space with 400 μL of the iPS-RPE cell suspension (2.4×10^6/mL) as per our previous reports [11, 12]. RPE cells were stained with fluorescent dye PKH (PKH26GL; fluorescent at 567 nm; Sigma-Aldrich) in order to trace the cells after the transplantation. The graft cells were monitored by color fundus photographs, fluorescence angiography (FA: both RetCamII and Clarity), and optical coherence tomography (OCT) (Nidek) at 1, 2, and 4 weeks after the surgery. To avoid visual loss in the subject animal, the transplantation site was positioned out of the macular region. In order to avoid infectious endophthalmitis related to the surgery, preoperative ocular disinfection treatment was performed. In all tested primates, transplantation of the fellow eye was carried out after confirming that there were no complications in the first eye at one week after surgery. For example, since there were no problems found during the medical examination of the right eye of

the DrpZ12 monkey at one week after the initial surgery, we then performed left eye surgery. Subsequently, however, inflammation unexpectedly appeared in both eyes (at around 2 weeks). Although prior to the sacrifice there were no changes in the behavior of the monkey regarding daily routines, i.e., feeding and drinking water, the animal was sacrificed after taking into consideration the possibility of binocular visual impairment and the importance of the overall investigation.

Major histocompatibility complex (MHC) typing

Genotyping of MHC-1 and MHC-II genes in cynomolgus monkeys was performed by pyrosequencing as previously described[13]. MHC information for the 1121A1 MHC homozygote iPS-RPE cells, Cyn 46a RPE cells (MHC heterozygote: control), and the TLHM-6 monkey (MHC-mismatched monkey) has been described in our previously published report[11]. **Supplementary Table 1** shows the MHC profiles of the MHC-matched monkeys (DrpZ11 and DrpZ12).

Polymerase chain reaction (PCR) and basic local alignment search tool (BLAST) analysis

DNA was extracted from the samples using a DNA Mini Kit (Qiagen). Genomic DNA of bacteria, fungi, and mycoplasma in the iPS-RPE cells and vitreous fluids was measured using real-time quantitative PCR assays. PCR was performed using a LightCycler 480 II instrument (Roche). The primers and probes (targeting the DNA of the region encoding the 16S ribosomal RNA (16S ribosomal DNA) used in this study for detection of mycoplasma-DNA were purchased from Nihon Techno Service Co., Ltd. (Tokyo, Japan). These samples were used for the quantitative PCR analysis. The Hokkaido System Sciences Co., Ltd., was contracted to perform the BLAST analysis. DNA was sequenced and aligned with data available from the GenBank at the National Institutes of Health with BLAST, a computer alignment program. After the alignment

results for the 16s ribosomal RNA gene were matched to the database, the homology analysis was then performed.

Detection of anti-mycoplasma antibody in the serum from mycoplasma-infected monkey

Sera (n=2) of the DrpZ12 monkey that was transplanted with mycoplasma-infected iPS-RPE cells were collected. The first sample was obtained prior to surgery, while the other was collected at 4 weeks after the transplantation. Cultured monkey iPS-RPE cells (1121A1) that were infected with mycoplasma and primary monkey RPE without infection (1×10^4 cells/well) were re-cultured in a 96-well culture plate. As per our previous report [12], RPE cells were incubated with the serum (×50 with PBS) overnight at 4°C. The cells were then incubated with DAPI (×1000; Invitrogen) and a secondary antibody Alexa Fluor 488 anti-human IgG (×2000; Invitrogen) for 1 h at room temperature. Primary RPE cells were used as the control. Images were acquired with a confocal microscope (LSM700, Zeiss). Relative fluorescence intensity was analyzed using image analysis software (ZEN, Zeiss). At least three independent experiments were performed for the *in vitro* data. To test the fluorescence intensity difference, statistical analyses were performed using the paired Student's t-test. Values were considered statistically significant if $p < 0.05$.

Mixed lymphocyte-RPE assay with iPS-RPE cells and blood cells, and flow cytometry

Peripheral blood mononuclear cells (PBMC) were isolated from a healthy adult MHC control monkey donor (DrpZ11), with the allogeneic immune responses assessed for the proliferation by Ki-67 incorporation in the PBMC. PBMC were cultured with MHC-matched 1121A1 iPS-RPE cells (mycoplasma infected or not). The culture medium used was RPMI-1640 medium containing 10% fetal bovine serum (BioWhittaker), human recombinant interleukin-2 (IL-2: Becton Dickinson), 10 mM

HEPES (Sigma), 0.1 mM nonessential amino acids (Sigma), 1 mM sodium pyruvate (Sigma), penicillin-streptomycin (Gibco), and 1×10^{-5} M 2-mercaptoethanol (Sigma). Before the assay, the RPE cells were irradiated (20 Gy). After 96–120 h, PBMC were analyzed by flow cytometry (Ki-67 proliferation assay by fluorescence-activated cell sorting [FACS]) [11]. For the Ki-67 proliferation assay by FACS analysis, the following antibodies were prepared: APC-labeled anti-CD4 (helper T cells: Miteny Biotec, #130-098-133), APC-labeled anti-CD8 (cytotoxic T cells: eBioscience, #17-0088), APC-labeled anti-CD11b (macrophages/monocytes: Milteny Biotec, #130-091-241), FITC-labeled anti-CD20 (B cells: Miteny Biotec, #130-091-108), APC-labeled anti-NKG2A (NK cells: Milteny Biotec, #130-098-812), and phycoerythrin (PE)-labeled anti-Ki-67 (BioLegend, #350504). The harvested PBMC were stained with the above antibodies at 4°C for 30 min. The intracellular staining for Ki-67 was performed after cell fixation and permeabilization (BioLegend). All samples were analyzed on a FACSCanto II Flow Cytometer (BD). Data were analyzed using FlowJo software (version 9.3.1).

***Immunohistochemistry* (IHC)**

Monkey eyes collected at 1 month were fixed and embedded in paraffin (Sigma-Aldrich). Paraffin sections were sliced into 10-μm thick sections. Detailed information on the procedure has been presented in our previous reports [11, 12]. The same immunochemical techniques and photographing methods, as mentioned below, were applied to all sections. Additional primary antibodies against the following proteins were used: ionized calcium-binding adapter molecule 1 (Iba1) (host: rabbit, ×1000; Wako, #019-19741), CD3 (host: rabbit, ×100; Abcam, #ab16669), MHC-II (host: mouse, ×100; Dako Cytomation, #Nr.M0775), Ly6G (host: rat ×100; Abcam, #ab25024), NKG2A (host: rabbit, ×100; Abcam, #ab93169) and Alexa Fluor 488 anti-Human IgG (host: goat, ×2000; Invitrogen, #A11013). All sections were incubated at 4°C overnight

198 with the pertinent primary antibodies[11, 12]. Images were acquired with a confocal
199 microscope (LSM700, Zeiss; http://www.zeiss.com).
200
201 ***Measurements of cytokines***
202 Vitreous fluids (160 to 200 μl) were collected from the transplanted left eye of the
203 monkey (TLHM-6) at the time of transplantation (0 weeks) and at 1, 2, and 4 weeks
204 after transplantation. Cytokine array experiments on the vitreous fluids were conducted
205 at Filgen Incorporated (Nagoya, Japan) using the Monkey Cytokine Magnetic 29-Plex
206 Panel (Thermo Fisher Scientific). The measurement proteins were EGF, eotaxin,
207 FGF-basic, G-CSF, GM-CSF, HGF, IFN-γ, IL-1β, IL-1RA, IL-2, IL-4, IL-5, IL-6, IL-8,
208 IL-10, IL-12, IL-15, IL-17, I-TAC, MCP-1, MDC, MIF, MIG, MIP-1α, MIP-1β,
209 RANTES, TNF-α, VEGF, and IP-10.
210
211

Results

Case 1: Severe ocular inflammation in MHC-matched iPS-RPE cell transplantation

In the first step, we transplanted MHC homozygous iPS-RPE cells (1121A1 lines: cell suspension) into a MHC heterozygote, which in this case was the MHC-matched monkey (right eye of the DrpZ12 monkey). All clinical symptoms were followed after the initial transplantation. At 2 weeks after the transplantation, a whitish infiltrating mass was found in the subretinal space at the site of the graft (**Fig. 1A**). FA images clearly showed that there was fluorescence leakage in the retinal vein on the bleb of the grafted site (**Fig. 1B**). OCT evaluations indicated that there were deposits under the retina and subretinal fluids (**Fig. 1C**). At 4 weeks after the transplantation, vitreous opacity caused the fundus to be invisible (**Supplementary Fig. 1A**). At postoperative day 33, fibrin was seen in the anterior chamber and iris rubeosis was also observed (**Supplementary Fig. 1B**).

Although the vitreous and retina in the eyeball of the DrpZ12 monkey were clouded due to vitreous hemorrhage (**Supplementary Fig. 1C**), the retina and vitreous were transparent in the control monkey eye (**Supplementary Fig. 1D**). After removal of the vitreous, retinal hemorrhage was observed in the retina (**Fig. 1D**).

To examine inflammation by IHC, we conducted hematoxylin and eosin (H&E) staining and immune staining of inflammatory cells in the retinal sections. H&E staining revealed the presence of hemorrhagic retinal detachment and retinal hemorrhage, which suggested a retinal circulation disorder (**Fig. 1E**). Results also showed there was a large amount of inflammatory cell infiltration centered on the site of the graft along with choroidal vasodilation (**Fig. 1F**). Immune staining additionally revealed large infiltrations of $Iba1^+$ cells, MHC class II^+ cells, $CD3^+$ cells, $Ly6G^+$ cells, and $NKG2A^+$ cells on the site of the graft (**Fig. 1G**). In addition, deposits of IgG were also noted at the graft site (**Fig. 1G**). The left eye, which underwent the transplantation

239 at 1 week after the right eye also exhibited similar findings, thereby indicating that the
240 transplanted eye also had severe ocular inflammation (**Supplementary Fig. 2**).
241
242 **Case 2: Severe ocular inflammation in MHC-mismatched iPS-RPE cell**
243 **transplantation**
244 We also observed a case of severe inflammation at the transplanted site after
245 MHC-mismatched iPS-RPE transplantation in a primate. Although remarkable changes
246 were observed in the color fundus photographs at 2 weeks after the transplantation (**Fig.**
247 **2A**), FA showed there were fluorescence leakages in the grafted area and the macula
248 (**Fig. 2B**). A high signal deposit under the retina was observed in the OCT images (**Fig.**
249 **2C**). H&E staining showed that there were infiltrating cells in the subretinal space of the
250 transplanted area. Similar to the first case, we also found choroidal vasodilation (**Fig.**
251 **2D**). IHC of the infiltrating cells collected at the grafted site revealed infiltration of
252 $Iba1^+$ cells, $CD3^+$ cells, MHC class II^+ cells, $Ly6G^+$ cells, IgG^+ tissues, and $NKG2A^+$
253 cells (**Fig. 2E**).
254 Subsequently, we then investigated the differences in inflammation between the
255 mycoplasma infection and post-transplant immune rejections after IPS-RPE cell
256 transplantation (w/o infection). We used IHC to examine the anti-Ly6G (neutrophil) and
257 anti-NKG2A (NK cells) in the retinal sections of a monkey that had immune attacks
258 after iPS-RPE transplantation and in a normal control monkey. In the RPE-related
259 rejection retina, although infiltrating cells were primarily observed along the grafts,
260 $Ly6G^+$ and $NKG2A^+$ cells were not found in these areas (**Fig. 3A**). In addition, there
261 were also no $Ly6G^+$ and $NKG2A^+$ cells observed in the normal control retina (**Fig. 3B**).
262
263 **Detection of mycoplasma genomic DNA from donor iPS-RPE cells and recipient**
264 **vitreous samples**
265 Since ocular inflammation was fulminant as compared to the RPE cells-related rejection

that we observed in our previous studies [11, 12], we suspected this inflammation was due to an infection caused by microorganisms. Quantitative PCR has been previously performed using primers and probes for detecting bacterial 16S rDNA [1], fungal 28S rDNA [14], and mycoplasma species. In the present study, we prepared DNA from stocks of transplanted iPS-RPE cells (1121A1 or 46a lines). We detected 2.27×10^{10} copies/μg·DNA of mycoplasma-DNA from the 1121A1 iPS-RPE cells, while 9.82×10^{9} copies/μg·DNA were detected from the 46a iPS-RPE cells. We also demonstrated that bacteria 16S rDNA of the mycoplasma species was positive, while 16S rDNA of the other bacteria species and fungi 28S rDNA were not detected (data not shown). Interestingly, there was no obvious difference in the optical microscopic findings between the mycoplasma non-infected and infected iPS-RPE cells (**Fig. 4A**). We also performed quantitative PCR of vitreous fluids, and detected 7.37×10^{4} copies/mL of mycoplasma-DNA in samples from the right eye at 2 weeks after transplantation and 1.80×10^{4} copies/mL from the left eye at 1 week after transplantation (**Fig. 4B**). Homology analysis using the BLAST database for the 16S rRNA gene in the infected iPS-RPE cells detected a homology of 99.276 to 99.783% with the strain of *Mycoplasma arginini* (*M. arginini*) (**Table 1**). In addition, vitreous fluids from the recipient monkeys also exhibited similar results (**Table 1**).

Detection of mycoplasma specific antibodies in recipient sera

In order to demonstrate that mycoplasma-specific antibody was produced in the recipient by the mycoplasma infection, in the next step we conducted immune staining of mycoplasma-infected and non-infected iPS-RPE cells using sera. The sera were collected before transplantation and at 4 weeks after transplantation from the recipient monkeys (DrpZ12). Nuclei of the non-infected cells were clearly stained with DAPI. In infected cells, in addition to the cell nuclei, nonspecific staining between and around the nuclei of RPE cells was also observed (**Fig. 4C**). Immunocytochemistry with

fluorescently labeled anti-IgG antibody tended to show that the intensity of fluorescence in the infected iPS-RPE cells was much higher than that for the non-infected cells. In the infected iPS-RPE cells, fluorescent intensity for the serum at 4 weeks was significantly higher than that seen for the baseline serum (P = 0.021, **Fig. 4D**). Thus, we suspected that mycoplasma-specific antibody might be present in the serum following the initial transplantation.

Inflammatory cells respond to mycoplasma-infected iPS-RPE cells *in vitro*

To investigate whether mycoplasma stimulates the immune responses, we analyzed PBMC by the mixed lymphocyte-RPE assay. When PBMC from the DrpZ11 MHC-matched monkey were co-cultured with MHC-matched 1121A1 iPS-RPE cells, there was clear suppression of the proliferation as compared to that observed for the culture of the control PBMC alone (**Fig. 5A**). On the other hand, when PBMC from the DrpZ11 monkey were co-cultured with mycoplasma-infected 1121A1 iPS-RPE cells, there was clear enhancement of the proliferation as compared to the cultures with PBMC only, i.e., all types of the inflammatory cells responded against the RPE cells *in vitro* (**Fig. 5B**).

Increased various inflammatory cytokines and chemokines from vitreous in mycoplasma-infected iPS-RPE cell transplantation

To examine whether ocular fluids in the mycoplasma-infected iPS-RPE cell transplantation monkey (TLHM-6) contain inflammatory cytokines and chemokines, we collected vitreous fluids at 0, 1, 2, and 4 weeks after transplantation. After collection, we then measured the inflammatory proteins using the cytokine beads array. Among the 29 proteins tested, significant increases were observed in the IL-1β, IL-1RA, IL-6, IL-12, IL-15, IFN-γ, MIF, eotaxin, IP-10, I-TAC, MCP-1, MDC, MIG, RANTES, and VEGF (**Table 2**). As compared to the vitreous data obtained before surgery (0 weeks),

there was a significant increase in the Th1-related cytokines (IL-12, IL-15, and IFN-γ) and Th1-related chemokines (IP-10, I-TAC, MIG, and RANTES) in the mycoplasma-infected vitreous samples, especially at 1 or 2 weeks after transplantation (**Table 2**). These results indicated that various inflammatory cytokines/chemokines presented in the retina and vitreous (similar to a "cytokine storm" in the eye).

Taken together, the *in vivo* and *in vitro* results demonstrated that mycoplasma-infected iPS-RPE cells can stimulate immune responses, thereby causing severe inflammation in the recipient eye after transplantation.

Discussion

Results of the present study showed that severe inflammation mainly occurred within the grafted area, especially in the subretinal space and choroid, with the inflammation then spreading throughout the eyeballs. These results suggested that the mycoplasma that directly invades the eye may cause strong immune responses. Moreover, the mixed lymphocyte-RPE assay showed that MHC-matched iPS-RPE cells suppressed proliferation of inflammatory cells, whereas RPE cells infected with mycoplasma enhanced the proliferation of inflammatory cells *in vitro*. These results demonstrate that mycoplasma can cause inflammatory reactions.

We performed quantitative PCR in order to try and detect mycoplasma *spp* DNA collected from ocular samples and explanted RPE cells. In addition, we also tried to identify the species of the mycoplasma using homology analysis of the amplified 16S ribosomal DNA with the BLAST database. We detected more than a 99% homology with the strain of *M. arginini*. It has been previously reported that a 98.7% homology to 16S ribosomal DNA corresponded to the criterion of the 70% of the DNA-DNA hybrid, which has been considered to be the conventional standard of judgment for species [15]. Based on these findings, the mycoplasma that infected the iPS-RPE cells and inflamed eyeballs was judged to be *M. arginini*. It has been previously reported that *M. arginini* is one of major species that causes contamination of cell cultures [16]. Furthermore, it has been suggested that PCR can be useful for the early diagnosis of *Mycoplasma hominis* infections that occur after cardiac chest transplantations[8]. Since these infections are known to progress with the passage of time, a rapid diagnosis is important in order to be able to provide an effective treatment. In some species, however, it can often be difficult to successfully perform cultures. Moreover, we also showed that the optical microscopic findings indicated that there was no obvious change in the iPS-RPE cells infected with *M. arginini*. Thus, when trying to detect microorganisms in a clinic, rapid diagnostic tests such as PCR are necessary.

As shown in the present study, mycoplasma-infected cells caused intensive ocular inflammation when the cells were placed in the subretinal space of the recipient's eye. Initial signs included retinal vasculitis and subretinal fluorescence leakages upon FA examination, while OCT revealed there was subretinal inflammatory cell infiltration at the grafted area. In addition, we also observed retinal hemorrhage and iris rubeosis, which indicates the presence of an impaired retinal circulation. Furthermore, these severe inflammatory findings suggested that intraocular invasion by mycoplasma might lead to a poor prognosis for visual function. Ocular inflammation can also develop in humans in association with *M. pneumoniae* infection. Several cases have also been reported in patients found to have edema of the optic papilla or anterior uveitis [4]. There are also studies that have reported finding retinal inflammation and circulatory disorders, including a case with panuveitis accompanied by retinal hemorrhage [6], and a case with frosted branch angiitis and macular edema [5]. The inflammation and hemorrhage in both cases were mild, with no decrease in the final visual acuity observed. Recently, Narita classified the pathology of mycoplasma infection into three categories that included, 1) a direct type in which the mycoplasma directly invades the lesion part, 2) a vascular occlusion type due to vasculitis, and 3) an indirect type such as an autoimmune reaction. The author considered that these three elements overlapped to form the overall disease state [17]. In human uveitis cases, the mycoplasma antigen has yet to be detected in any eyes. Thus, the pathology of the mycoplasma-related ocular inflammation cases in humans may reflect the indirect type. In a rodent model in which mycoplasma was directly administered intraocularly, the animals exhibited severe endophthalmitis-like symptoms such as choroidal edema and exudative retinal detachment [2, 3]. Due to the fact that both our present cases and this rodent mycoplasma model exhibited severe ocular inflammation, this suggests that both of these can be classified as examples of direct type infections.

The entire genome of *M. arginini*, which was detected in our present cases, has

been previously analyzed. Overall, it is thought that the virulence of *M. arginini* in living organisms is low, as it lacks the capsular synthetic genes and active oxygen production genes that are considered to be the cause of pathogenicity for mycoplasma [18]. However, the findings for our present cases revealed that mycoplasma caused severe intraocular inflammation and circulatory disorder by means other than a capsule and active oxygen. Moreover, our *in vitro* experiments additionally revealed that mycoplasma has the ability to stimulate inflammatory cells. In the MLR assay, non-infected iPS-RPE cells suppressed proliferation of inflammatory cells such as $CD4^+$ T helper cells, $CD8^+$ cytotoxic T cells, $CD11b^+$ monocytes/microglia, $CD20^+$ B cells, and $NKG2A^+$ NK cells. Conversely, in the mycoplasma-infected iPS-RPE cells, the proliferation of these inflammatory cells was greatly enhanced. It has been shown that *M. arginini* both stimulates human PBMC to produce IL-1β, IL-6, and TNF-α [19] and causes mesenchymal stem cells to produce complement factors [20]. Mycoplasma does not produce toxins, unlike other bacteria, but the cell membrane lipoproteins of mycoplasma can cause an immune response via TLR2, 4 and autophagy[21]. The findings of these previous reports support the concept that mycoplasma directly stimulates leukocytes, thereby initiating the inflammatory responses by a mechanism that differs from the other bacteria. In contrast, RPE infected with chlamydia has been reported to be able to upregulate secretion of IL-8[22], IL-6, and VEGF[23]. Thus, mycoplasma infection might also have influenced the cytokine production of RPE cells, thereby enhancing the ocular inflammation and neovascularization in our current study cases.

In our present cases, infiltration of inflammatory cells including $Ly\text{-}6G^+$ cells and $NKG2A^+$ cells were observed in the grafted area. In the retina of the post-transplant immune rejections, although $Iba1^+$ cells, MHC class II^+ cells and $CD3^+$ T cells invaded the grafted area, [11] $Ly6G^+$ cells and $NKG2A^+$ cells were not found. Infiltration of neutrophils is known to be a characteristic pathological finding in lungs with *M.*

410 *pneumoniae* pneumonia[24]. Resistance to mycoplasma has been shown to be mediated by
411 activated natural killer cells [25]. The presence or absence of infiltrating $Ly6G^+$ cells and
412 $NKG2A^+$ cells may reflect the difference in the pathophysiology between mycoplasma
413 infection and immune rejection.

414 The importance of taking precautionary measures to prevent mycoplasma
415 contamination into cells that will be used for transplantation has been recognized, with
416 mycoplasma testing now defined within the pharmacopoeia of several countries[26, 27].
417 For human retinal cell transplantations, multiple sterility tests for mycoplasma have
418 been recommended[28]. However, the possibility still exists that mycoplasma ocular
419 infection could potentially occur by accident. Thus, the importance of our current
420 research is that it provides additional knowledge that is necessary for diagnosing cases
421 of mycoplasma ocular infection.

422 In the present study, although we did not consider using any treatments in the
423 experimental animals, as the monkeys were to be sacrificed, it is likely that they
424 probably would have been unable to see due to the severe ocular inflammation.
425 Protocols using fluoroquinolones, tetracyclines, and macrolides have been proposed for
426 removing mycoplasmas that have infected cultured cells[29, 30]. Although quinolones,
427 macrolides, and tetracyclines are conventionally considered to be effective for
428 mycoplasma infections in humans, the proportion of mycoplasmas that are resistant to
429 quinolones and macrolides is increasing[31, 32]. Therefore, cases that are difficult to treat
430 are becoming more of a problem. There have been a few reports regarding the use of
431 doxycycline to treat *M. arginini*-infected humans[33, 34]. However, presently the number
432 of cases reported is small and as of yet, the drug resistance remains unknown. To our
433 knowledge, there have yet to be any reports on the efficacy and safety of these
434 antibiotics in the intraocular infections caused by mycoplasma. Furthermore,
435 verification using an infected animal model is also necessary in order to develop a

436 treatment protocol. Since transplantation using MHC-matched primates can be used to
437 help avoid inflammation and potential immune rejections[11], this model is considered to
438 be useful for studies on infection, as this may make it possible to specifically analyze
439 the mechanism responsible for inflammation due to infection.

440 This is the first study to show that mycoplasma-infected explanted cells are able to
441 cause severe ocular inflammation. Circulatory insufficiency caused by inflammation
442 and thrombosis, followed by angiogenesis might be associated with the pathological
443 mechanisms responsible for mycoplasma intraocular inflammation. In fact, the present
444 study demonstrated the presence of retinal and vitreous hemorrhages in an eye in
445 conjunction with a large number of inflammatory cells. Therefore, the present results
446 highlight the potential problem of infections that might be associated with
447 transplantations, such as during regenerative medicine-associated cell-based therapy.
448

Acknowledgements

We thank N. Hayashi, K. Iseki, S. Fujino, and M. Kawahara (Laboratory for Retinal Regeneration, RIKEN BDR, Kobe, Japan) for their expert technical assistance.

454 **References**

455 1. Sugita S, Shimizu N, Watanabe K, et al. Diagnosis of bacterial endophthalmitis
456 by broad-range quantitative PCR. *Br J Ophthalmol* 2011;95:345-349.
457 2. Pavan-Langston D. Mycoplasmal anterior and posterior uveitis. I. Clinical
458 manifestations of the experimental disease. *Arch Ophthalmol* 1969;82:245-252.
459 3. Pavan-Langston D. II. Histopathologic manifestations of mycoplasmal uveitis.
460 *Arch Ophthalmol* 1969;82:253-258.
461 4. Liu EM, Janigian RH. Mycoplasma pneumoniae: the other masquerader. *JAMA*
462 *Ophthalmol* 2013;131:251-253.
463 5. Matsou A, Riga P, Samouilidou M, Dimitrakos S, Anastasopoulos E. Bilateral
464 intermediate uveitis with appearance of frosted branch angiitis and association with
465 Mycoplasma pneumoniae infection: case report and review of the literature. *J AAPOS*
466 2016;20:358-361.
467 6. Yashar SS, Yashar B, Epstein E, Viani RM. Uveitis associated with
468 Mycoplasma pneumoniae meningitis. *Acta Ophthalmol Scand* 2001;79:100-101.
469 7. Gass R, Fisher J, Badesch D, et al. Donor-to-host transmission of Mycoplasma
470 hominis in lung allograft recipients. *Clin Infect Dis* 1996;22:567-568.
471 8. Sampath R, Patel R, Cunningham SA, et al. Cardiothoracic Transplant
472 Recipient Mycoplasma hominis: An Uncommon Infection with Probable Donor
473 Transmission. *EBioMedicine* 2017;19:84-90.
474 9. Marini H, Merle V, Frebourg N, et al. Mycoplasma hominis wound infection
475 after a vascular allograft. *J Infect* 2008;57:272-274.
476 10. Rottem S, Naot Y. Subversion and exploitation of host cells by mycoplasmas.
477 *Trends Microbiol* 1998;6:436-440.
478 11. Sugita S, Iwasaki Y, Makabe K, et al. Successful Transplantation of Retinal
479 Pigment Epithelial Cells from MHC Homozygote iPSCs in MHC-Matched Models.
480 *Stem Cell Reports* 2016;7:635-648.
481 12. Sugita S, Makabe K, Fujii S, et al. Detection of Retinal Pigment
482 Epithelium-Specific Antibody in iPSC-Derived Retinal Pigment Epithelium
483 Transplantation Models. *Stem Cell Reports* 2017;9:1501-1515.
484 13. Shiina T, Yamada Y, Aarnink A, et al. Discovery of novel MHC-class I alleles
485 and haplotypes in Filipino cynomolgus macaques (Macaca fascicularis) by
486 pyrosequencing and Sanger sequencing: Mafa-class I polymorphism. *Immunogenetics*
487 2015;67:563-578.
488 14. Ogawa M, Sugita S, Watanabe K, Shimizu N, Mochizuki M. Novel diagnosis
489 of fungal endophthalmitis by broad-range real-time PCR detection of fungal 28S

ribosomal DNA. *Graefes Arch Clin Exp Ophthalmol* 2012;250:1877-1883.
15. Stackebrandt E, Ebers J. Taxonomic parameters revisited : tarnished gold standards. *Microbiology today* 2006;33:152-155.
16. Maniloff J, McElhaney RN, Finch LR, Baseman JB. Mycoplasmas: Molecular Biology and Pathogenesis. In: McGarrity G (ed), *Mycoplasmas and tissue culture cells.* Washington DC: American Society for Microbiology Press; 1992:445-454.
17. Narita M. Classification of Extrapulmonary Manifestations Due to Mycoplasma pneumoniae Infection on the Basis of Possible Pathogenesis. *Front Microbiol* 2016;7:23.
18. Hata E. Complete Genome Sequence of Mycoplasma arginini Strain HAZ 145_1 from Bovine Mastitic Milk in Japan. *Genome Announc* 2015;3.
19. Kita M, Ohmoto Y, Hirai Y, Yamaguchi N, Imanishi J. Induction of cytokines in human peripheral blood mononuclear cells by mycoplasmas. *Microbiol Immunol* 1992;36:507-516.
20. Lee DS, Yi TG, Lee HJ, et al. Mesenchymal stem cells infected with Mycoplasma arginini secrete complement C3 to regulate immunoglobulin production in B lymphocytes. *Cell Death Dis* 2014;5:e1192.
21. Shimizu T. Inflammation-inducing Factors of Mycoplasma pneumoniae. *Front Microbiol* 2016;7:414.
22. Boiko E, Maltsev D, Savicheva A, et al. Infection of Human Retinal Pigment Epithelium with Chlamydia trachomatis. *PLoS One* 2015;10:e0141754.
23. Fujimoto T, Sonoda KH, Hijioka K, et al. Choroidal neovascularization enhanced by Chlamydia pneumoniae via Toll-like receptor 2 in the retinal pigment epithelium. *Invest Ophthalmol Vis Sci* 2010;51:4694-4702.
24. Chen Z, Shao X, Dou X, et al. Role of the Mycoplasma pneumoniae/Interleukin-8/Neutrophil Axis in the Pathogenesis of Pneumonia. *PLoS One* 2016;11:e0146377.
25. Lai WC, Bennett M, Pakes SP, et al. Resistance to Mycoplasma pulmonis mediated by activated natural killer cells. *J Infect Dis* 1990;161:1269-1275.
26. The ministry of health labour and welfare. Mycoplasma Testing for Cell Substrates used for the Production of Biotechnological/ Biological Products. *The Japanese pharmacopoeia 17th edition English version*; 2016:2460-2464.
27. The European Directorate for the Quality of Medicines and Healthcare. 2.6.7 Mycoplasmas. *Europian Pharmacopoeia 90*; 2017:188-193.
28. da Cruz L, Fynes K, Georgiadis O, et al. Phase 1 clinical study of an embryonic stem cell-derived retinal pigment epithelium patch in age-related macular degeneration.

526 *Nat Biotechnol* 2018;36:328-337.
527 29. Uphoff CC, Drexler HG. Elimination of Mycoplasma from infected cell lines
528 using antibiotics. *Methods Mol Med* 2004;88:327-334.
529 30. Uphoff CC, Drexler HG. Eradication of Mycoplasma contaminations from cell
530 cultures. *Curr Protoc Mol Biol* 2014;106:28 25 21-12.
531 31. Kikuchi M, Ito S, Yasuda M, et al. Remarkable increase in
532 fluoroquinolone-resistant Mycoplasma genitalium in Japan. *J Antimicrob Chemother*
533 2014;69:2376-2382.
534 32. Principi N, Esposito S. Macrolide-resistant Mycoplasma pneumoniae: its role
535 in respiratory infection. *J Antimicrob Chemother* 2013;68:506-511.
536 33. Sillo P, Pinter D, Ostorhazi E, et al. Eosinophilic Fasciitis associated with
537 Mycoplasma arginini infection. *J Clin Microbiol* 2012;50:1113-1117.
538 34. Watanabe M, Hitomi S, Goto M, Hasegawa Y. Bloodstream infection due to
539 Mycoplasma arginini in an immunocompromised patient. *J Clin Microbiol*
540 2012;50:3133-3135.
541
542
543

Footnote

[1]This work was supported by the Research Center Network for Realization of Regenerative Medicine from the Japan Agency for Medical Research and Development (AMED) and by the RIKEN Junior Research Associate Program. This work was also supported by a Scientific Research Grant (B, 18H02959) from the Ministry of Education, Culture, Sports, Science and Technology of Japan.

[2]Corresponding address: Dr. Sunao Sugita, Laboratory for Retinal Regeneration, Center for Biosystems Dynamics Research, RIKEN, 2-2-3 Minatojima-minamimachi, Chuo-ku, Kobe 650-0047, Japan. Tel: +81-78-306-3305; Fax: +81-78-306-3303; E-mail: sunaoph@cdb.riken.jp

[3]Abbreviations used in this paper: BLAST, basic local alignment search tool; FA, fluorescein angiography; H&E, hematoxylin and eosin; Iba1, ionized calcium-binding adapter molecule 1; IHC, immunohistochemistry; INL, inner nuclear layer; iPSCs, iPS cells; iPS-RPE, iPS cells-derived retinal pigment epithelial; MHC, major histocompatibility complex; *M. arginini, Mycoplasma arginini*; *M. pneumoniae, Mycoplasma pneumoniae*; OCT, optical coherence tomography; ONL, outer nuclear layer; PBMC, peripheral blood mononuclear cells; PCR, Polymerase chain reaction; 16S ribosomal DNA, the DNA of the region encoding the 16S ribosomal RNA; RPE, retinal pigment epithelium; RPE cells, retinal pigment epithelial cells

567 **Figure Legends**

568 **Figure 1. Inflammation after allogeneic transplantation of MHC homozygote**
569 **iPS-RPE cells into the subretinal space of the right eye of the MHC-matched**
570 **monkey.**

571 Without using immunosuppression, we transplanted monkey 1121A1 iPS-RPE cells (5
572 × 10^5 cells with single-cell suspension) into the subretinal space in the DrpZ12
573 MHC-matched monkey. (**A**) At 2 weeks (2W) after surgery, the fundus color photograph
574 revealed a white subretinal mass infiltrating at the site of the graft (arrow). (**B**)
575 Fluorescein angiography (FA: arrow) revealed the leakage from the retinal vein at the
576 grafted site. (**C**) Optical coherence tomography (OCT) showed the presence of cell
577 infiltration (arrow) in the subretinal space of the grafted site. Presence of subretinal fluid
578 was also seen (arrowhead). (**D**) Retinal hemorrhages were observed in split eyeballs
579 extracted from the DrpZ12 monkey. Scale bar, 1 cm. (**E**) H&E staining for histological
580 interpretation in the right eye of the DrpZ12. Retinal edema (arrowhead) and intraretinal
581 and subretinal hemorrhages (arrow) were observed in the macula. (**F**) Infiltration of
582 inflammatory cells in the subretinal space (arrow) and thickened choroid were observed
583 in the transplanted area. Scale bar, 200 μm. (**G**) The graft iPS-RPE cells were stained
584 with PKH in order to trace the cells after transplantation. Photomicrographs of the
585 specimens collected from the paraffin sections show labeling of infiltrating cells in the
586 DrpZ12 monkey retina in the right eye. The markers used included anti-ionized
587 calcium-binding adapter molecule 1 (Iba1) (microglia/macrophage marker), MHC class
588 II (MHC-II) (antigen presenting cell marker), CD3 (T cell marker), Ly6G (neutrophil
589 marker), NKG2A (NK cell marker) and IgG (antibody and B cell marker). Many
590 infiltrating cells were observed including $Iba1^+$ cells, $MHC\text{-}II^+$ cells, $CD3^+$ cells, $Ly6G^+$
591 cells, $NKG2A^+$ cells, and there were IgG deposits around the PKH-positive iPS-RPE
592 cell graft. Scale bar, 40 μm.
593

Figure 2. Inflammation after MHC-mismatched allogeneic transplantation in the normal monkey.

Monkey 46a iPS-RPE cells (5×10^5, single-cell suspension) were transplanted into the subretinal space of a normal monkey (TLMH-6) without using immunosuppression. (**A**) At 2 weeks after surgery of the left eye, the results of fundus color photo revealed no obvious abnormality at the grafted site or macula area (arrow). (**B**) FA revealed leakages from the subretinal space at the grafted site and macula (arrow). (**C**) OCT showed the presence of cell infiltration in the subretinal space of the grafted site (white arrow). (**D**) TLHM-6 was sacrificed at 33 days after transplantation. Infiltration of inflammatory cells in the subretinal space and a thickened choroid were observed within the grafted site. Scale bar, 100 μm. (**E**) Photomicrographs show immune staining of the infiltrating inflammatory cells in the grafted site. There were many infiltrating cells observed around the PKH^+ iPS-RPE cell grafts including $Iba1^+$ cells, $CD3^+$ cells, $MHC\text{-}II^+$ cells, IgG, $NKG2A^+$ cells and $Ly6G^+$ cells. Scale bar, 40 μm.

Figure 3. Immunohistochemistry of the eye in the iPS-RPE cells-related immune rejection and negative control monkeys. (**A**) Photomicrographs showing labeling of the K247 monkey retina (at 4 months after surgery) with Ly6G and NKG2A. There was an inflammatory nodule (arrow) due to rejection along with many infiltrating cells in the retina. However, $Ly6G^+$ cells (left: neutrophils) and $NKG2A^+$ cells (right: NK cells) were not seen. INL: inner nuclear layer; ONL: outer nuclear layer; RPE: retinal pigment epithelium (**B**) Although the DrpZ10 monkey underwent a vitrectomy, we only injected medium without RPE cells in this animal. Photomicrographs show labeling of the DrpZ10 monkey retina with Ly6G and NKG2A. We failed to find either $Ly6G^+$ cells (left) or $NKG2A^+$ cells (right). Scale bar, 40 μm.

Figure 4. Detection of mycoplasma genome and anti-mycoplasma antibodies in

mycoplasma-infected iPS-RPE cell transplantation.

(**A**) Optical microscopic findings of monkey iPS-RPE cells (1121A1 lines). There were no differences noted in the microscopic image between the mycoplasma non-infected (upper) and infected (lower) RPE cells. Scale bar, 100 μm. (**B**) We performed qPCR in order to detect the mycoplasma-DNA in the vitreous collected from the DrpZ12 monkey. Quantitative levels of mycoplasma DNA in the vitreous of the right eye (at 2 weeks after transplantation) were 7.37×10^4 copies/mL, while they were 1.80×10^4 copies/mL for the left eye (at 1 week after transplantation). (**C**) To detect anti-mycoplasma antibody from infected monkey's serum, IHC was performed on the infected iPS-RPE cells and control primary monkey RPE cells using the anti-IgG antibody. RPE cells were incubated with the DrpZ12 serum collected before 0 weeks (0W) and at 4 weeks (4W) after transplantation. Monkey primary RPE cells with no infection that were stained with the DrpZ12 serum at 0 and 4 weeks showed low intensity for the IgG staining, with the cell nuclei clearly stained with DAPI. Monkey iPS-RPE cells infected with mycoplasma incubated with DrpZ12 serum showed high intensity for the IgG staining. Nonspecific staining between and around the nucleus of RPE cells was observed in addition to cell nuclei staining with DAPI. Scale bar, 50 μm. (**D**) The graphs show the mean fluorescence intensity of the IgG staining. Open bars show the intensity of the primary RPE cells. Black bars show the intensity of the iPS-RPE cells with the mycoplasma infection. Fluorescence intensity of iPS-RPE cells with the mycoplasma infection incubated with the serum at 4 weeks was significantly higher than that observed for the control serum (0 weeks, $p=0.021$).

Figure 5. Mixed lymphocyte-RPE assay with fresh PBMC plus iPS-RPE cells.

In the mixed lymphocyte-RPE assay with allogeneic 1121A1 iPS-RPE cells, PBMC (2×10^6 cells/well in the DrpZ11 MHC-matched monkey) were cultured with allogeneic iPS-RPE cells for 5 days. Before the assay, iPS-RPE cells were irradiated with 20 Gy,

with 1×10^4 cells then cultured in a 24-well plate. (**A**) Mycoplasma-infected iPS-RPE cells, (**B**) Mycoplasma-non-infected iPS-RPE cells. Harvested PBMC were stained with anti-CD4, anti-CD8, anti-CD11b, anti-CD20, anti-NKG2A, anti-Ki-67, with each isotype control antibody at 4°C for 30 min. The samples were analyzed on a FACS flow cytometer. Numbers (%) in the scatterplots indicate double-positive cells.

655 **Table 1. Results of BLAST analysis of bacterial 16S rRNA genes.**

Strain/Sequence Name	RPE cells % identity	Vitreous % identity
Mycoplasma arginini strain EF-Hungary 16S ribosomal RNA gene, partial sequence; 16S-23S ribosomal RNA intergenic spacer, complete sequence; and 23S ribosomal RNA gene, partial sequence	99.783	99.783
Mycoplasma arginini strain 284F08 16S ribosomal RNA gene, partial sequence	99.493	99.493
Mycoplasma arginini strain ATCC 23243 16S ribosomal RNA gene, partial sequence; 16S-23S ribosomal RNA intergenic spacer, complete sequence; and 23S ribosomal RNA gene, partial sequence	99.421	99.421
Mycoplasma arginini strain D1 16S ribosomal RNA gene, partial sequence	99.421	99.421
Mycoplasma arginini strain CBER2012BHK clone 4 16S ribosomal RNA gene, partial sequence	99.421	99.421
Mycoplasma arginini strain G230 16S ribosomal RNA gene, partial sequence Mycoplasma arginini strain G230(T) 16S ribosomal RNA gene, partial sequence	99.349	99.349
Mycoplasma arginini gene for 16S ribosomal RNA, complete sequence, strain: G230	99.276	99.276
Mycoplasma arginini DNA, complete genome, strain: HAZ145_1 Range 1: 209977 to 211358	99.349	99.349
Mycoplasma arginini DNA, complete genome, strain: HAZ145_1 Range 2: 140812 to 142193	99.276	99.276
Mycoplasma arginini 16S ribosomal RNA gene, partial sequence	99.349	99.349
Mycoplasma arginini strain 4X 16S ribosomal RNA gene, partial sequence	99.276	99.276

656

657

658

659 **Table 2. Measurements of cytokines and chemokines from vitreous fluids in**
660 **mycoplasma-infected iPS-RPE cell transplantation monkey.**

Cytokine	0 W vitreous	1 W vitreous	2 W vitreous	4 W vitreous
IL-1β	0.41 (0.04)	1.29 (0.07)*	0.84 (0.14)*	0.48 (0.08)
IL-1RA	ND	3110.55 (127.16)*	1039.07 (25.65)*	48.47 (13.84)*
IL-2	ND	ND	ND	ND
IL-4	9.04 (0)	9.75 (0.61)	9.04 (1.06)	9.04 (0)
IL-5	0.29 (0.06)	0.35 (0.06)	0.31 (0.06)	0.29 (0.06)
IL-6	1.44 (0.26)	710.23 (24.39)*	41.59 (3.25)*	3.44 (0.61)*
IL-8	3.72 (1.24)	5.23 (0.61)	4.52 (1.33)	3.30 (0.92)
IL-10	5.80 (0.39)	6.90 (0.67)	6.28 (0.88)	6.11 (0.65)
IL-12	19.84 (16.1)	40.78 (5.95)	162.81 (23.36)*	53.54 (15.42)
IL-15	ND	24.63 (10.03)*	24.14 (13.16)*	ND
IL-17	ND	ND	ND	ND
IFN-γ	ND	3.34 (2.31)	29.04 (3.53)*	ND
TNF-α	ND	0.38 (0.33)	0.38 (0.66)	0.00 (0.4)
MIF	ND	367.8 (15.52)*	404.87 (28.73)*	142.25 (11.8)*
Eotaxin	0.71 (0.11)	2.76 (0.29)*	2.35 (0.49)*	2.69 (0.37)*
IP-10	ND	Over	Over	240.8 (9.22)*
I-TAC	7.87 (1.06)	1056.86 (62.91)*	713.76 (16.07)*	21.09 (3.1)*
MCP-1	40.36 (9.88)	3883.63 (178.33)*	2738.51 (3.83)*	736.93 (24.48)*
MDC	ND	ND	82.11 (38.15)*	ND
MIG	ND	268.44 (14.2)*	420.21 (13.91)*	ND
MIP-1α	ND	ND	ND	ND
MIP-1β	ND	ND	9.66 (6.4)	ND
RANTES	ND	ND	19.9 (1.68)*	ND
EGF	ND	ND	ND	ND
FGF-basic	2.00 (0.68)	3.17 (1.13)	3.02 (1.55)	2.00 (0.85)
G-CSF	26.17 (6.45)	39.63 (7.84)	37.01 (12.24)	30.31 (6.29)
GM-CSF	1.14 (0.19)	1.36 (0.14)	1.31 (0.26)	1.14 (0.28)
HGF	ND	ND	ND	ND
VEGF	0.12 (0.08)	0.93 (0.12)*	0.34 (0.14)	0.03 (0.04)

661 Data are means (standard deviation) of three cytokine array determinations, pg/ml.
662 *P<0.05, t-test compared to data of the vitreous at 0 W.
663 W: weeks after transplantation; over: high value over the measurable range; ND: not
664 detected.

Figure 1

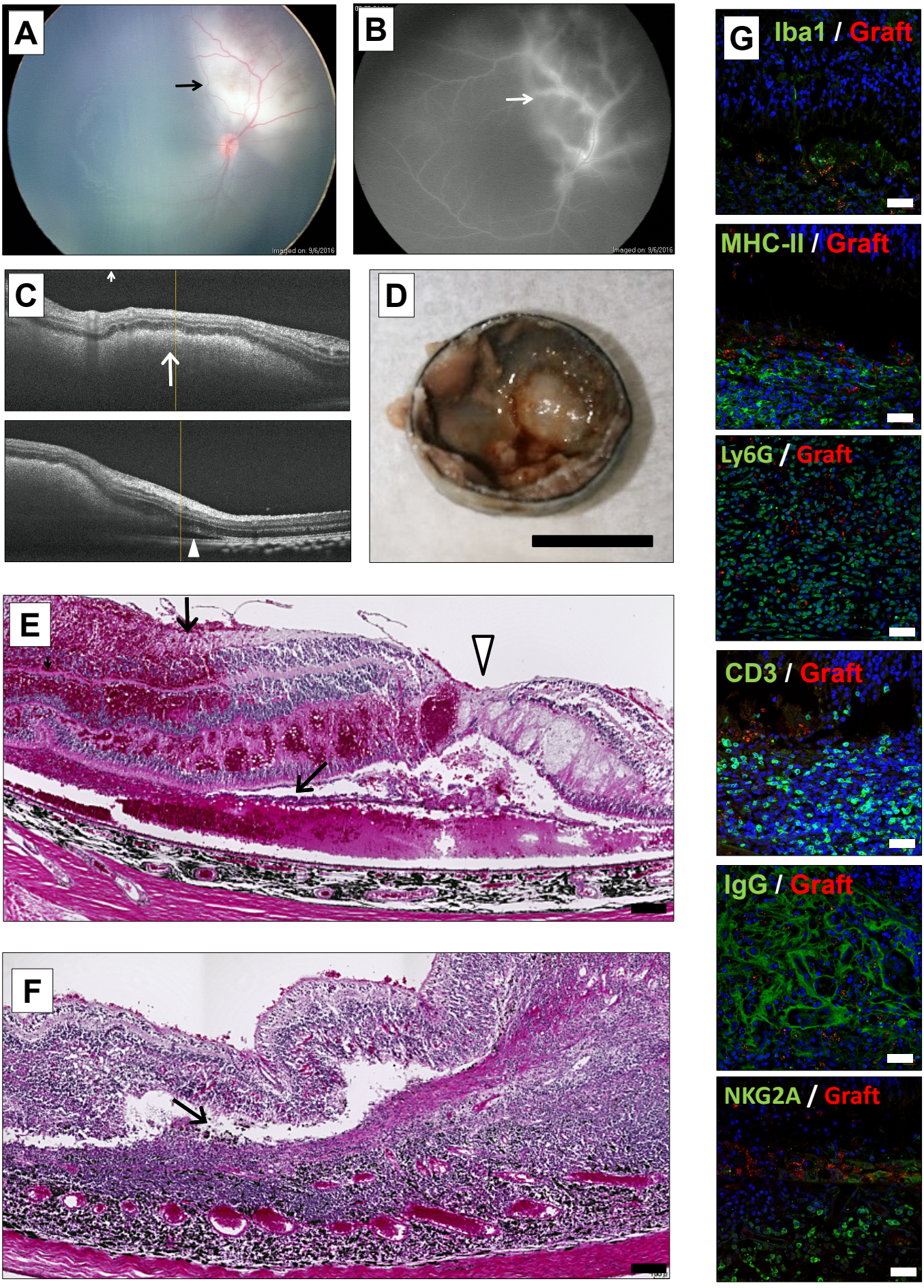
A
B
C
D
E
F
G
Iba1 / Graft
MHC-II / Graft
Ly6G / Graft
CD3 / Graft
IgG / Graft
NKG2A / Graft

Figure 2

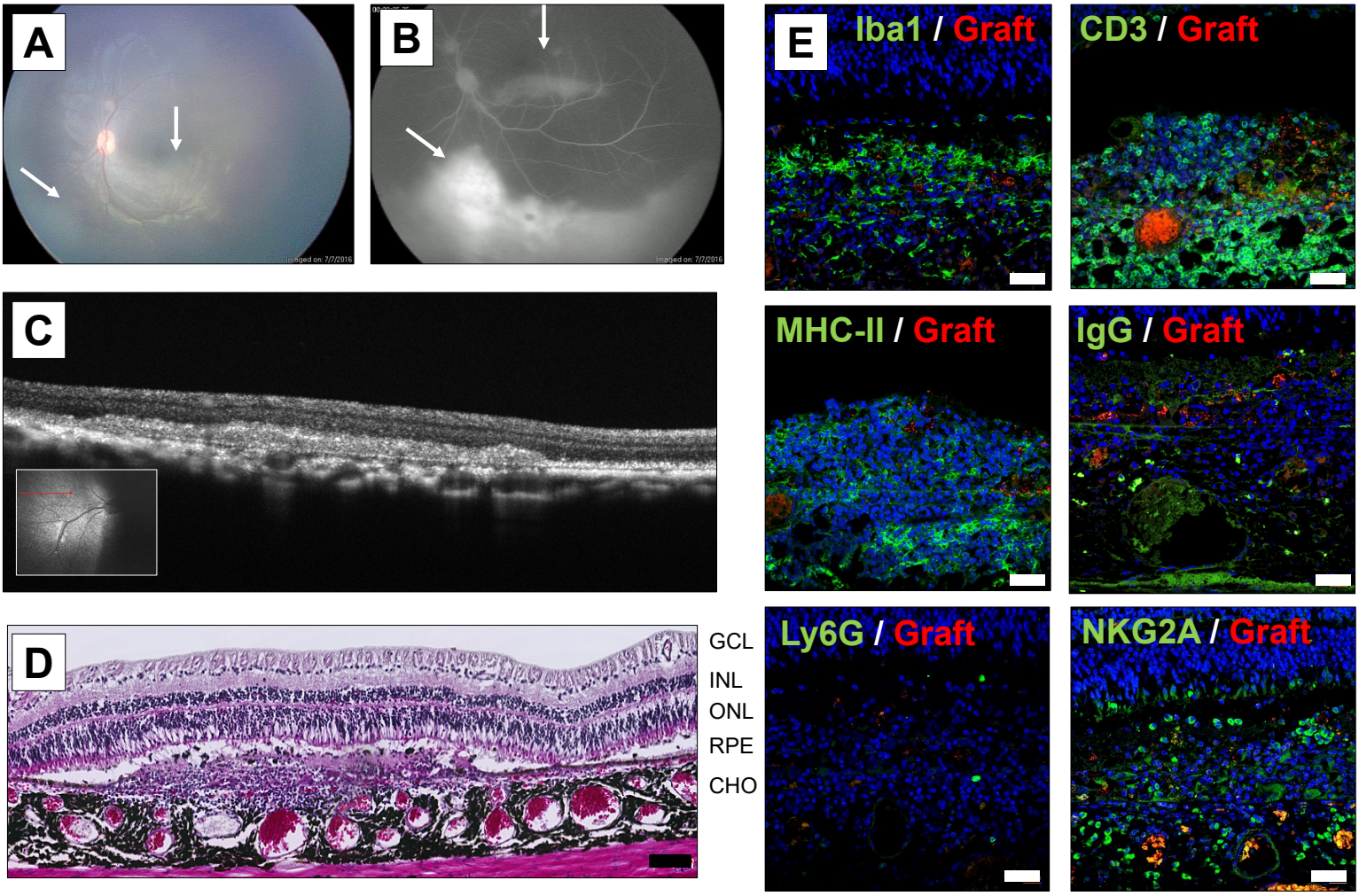
A
B
C
D
GCL
INL
ONL
RPE
CHO
E
Iba1 / Graft
CD3 / Graft
MHC-II / Graft
IgG / Graft
Ly6G / Graft
NKG2A / Graft

Figure 3

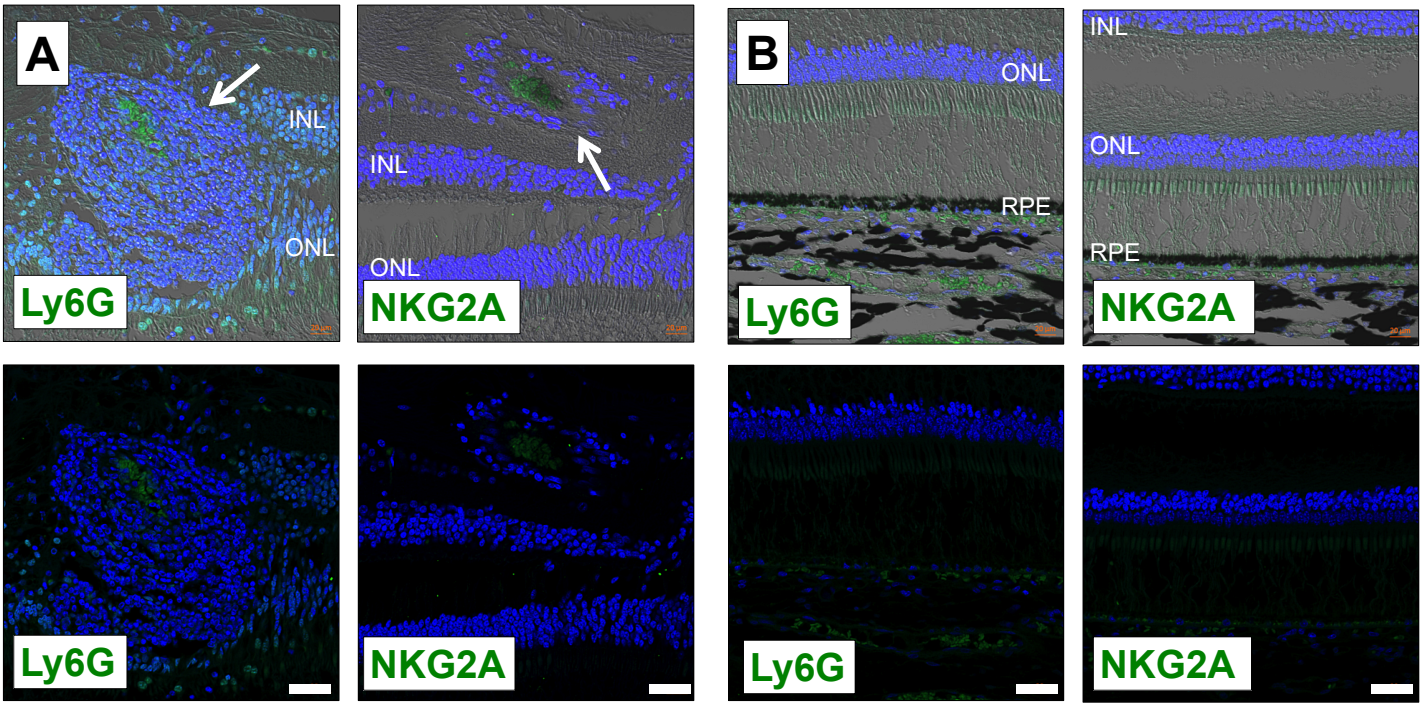
A
INL
ONL
Ly6G
INL
ONL
NKG2A
B
ONL
RPE
Ly6G
INL
ONL
RPE
NKG2A
Ly6G
NKG2A
Ly6G
NKG2A

Figure 4

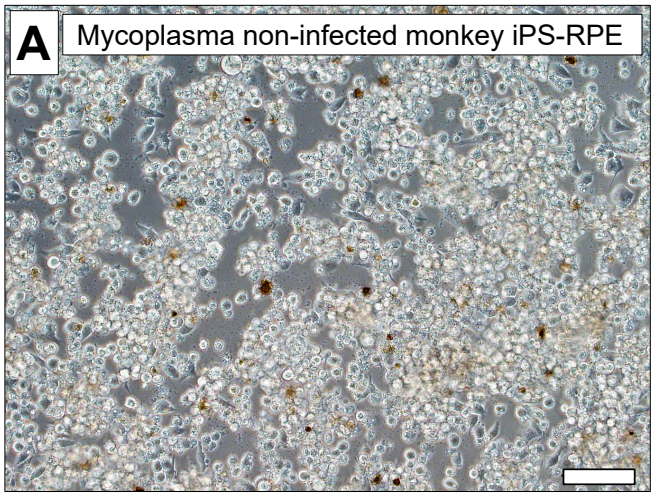
A
Mycoplasma non-infected monkey iPS-RPE

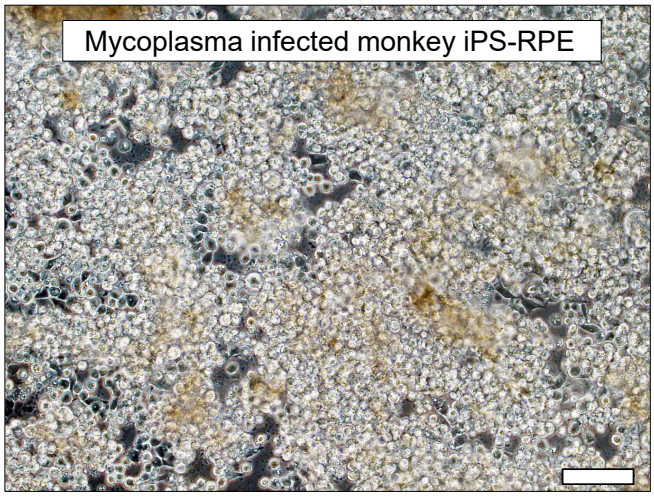
Mycoplasma infected monkey iPS-RPE

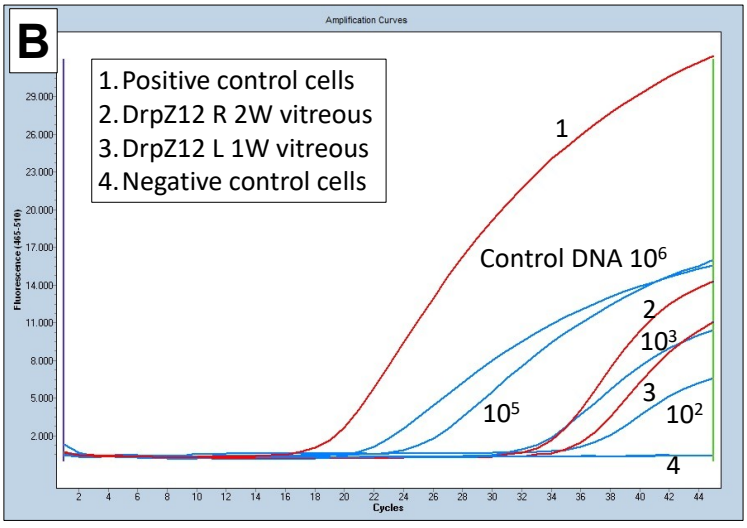
B
Amplification Curves
1. Positive control cells
2. DrpZ12 R 2W vitreous
3. DrpZ12 L 1W vitreous
4. Negative control cells
1
Control DNA 10^6
2
10^3
3
10^5
10^2
4
Fluorescence (465-510)
Cycles

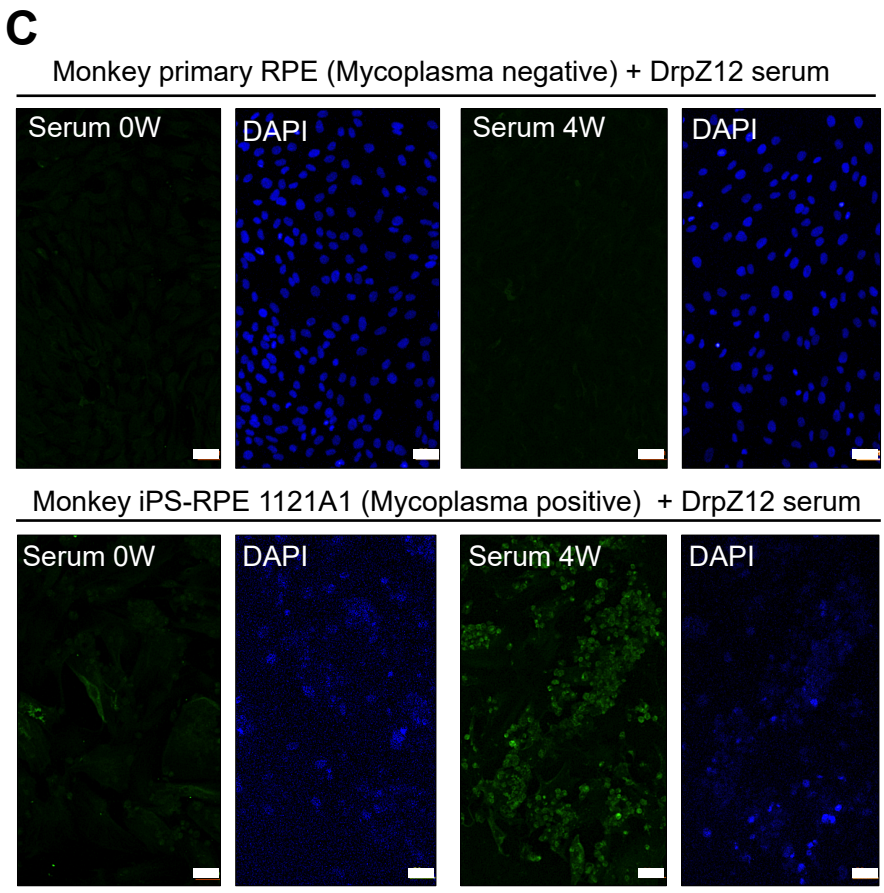
C
Monkey primary RPE (Mycoplasma negative) + DrpZ12 serum
Serum 0W
DAPI
Serum 4W
DAPI
Monkey iPS-RPE 1121A1 (Mycoplasma positive) + DrpZ12 serum
Serum 0W
DAPI
Serum 4W
DAPI

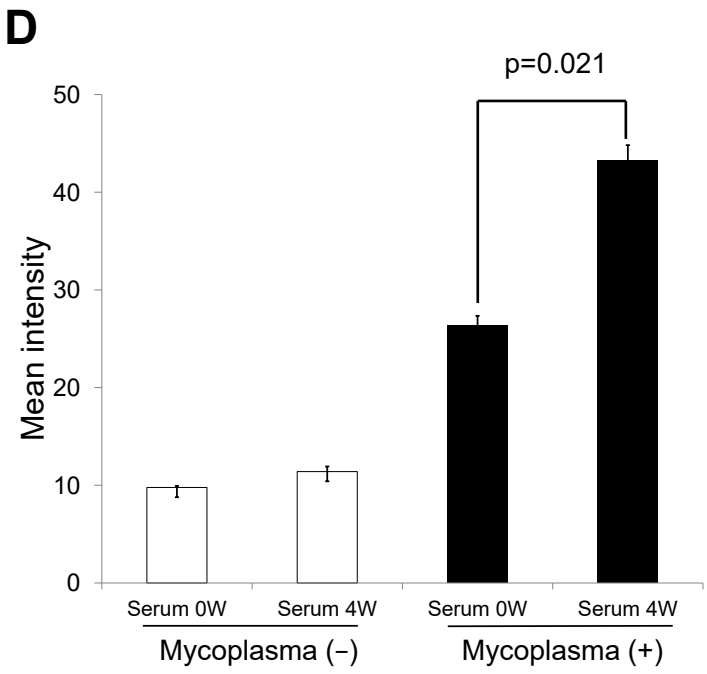
D
p=0.021
Mean intensity
50
40
30
20
10
0
Serum 0W
Serum 4W
Serum 0W
Serum 4W
Mycoplasma (−)
Mycoplasma (+)

Figure 5

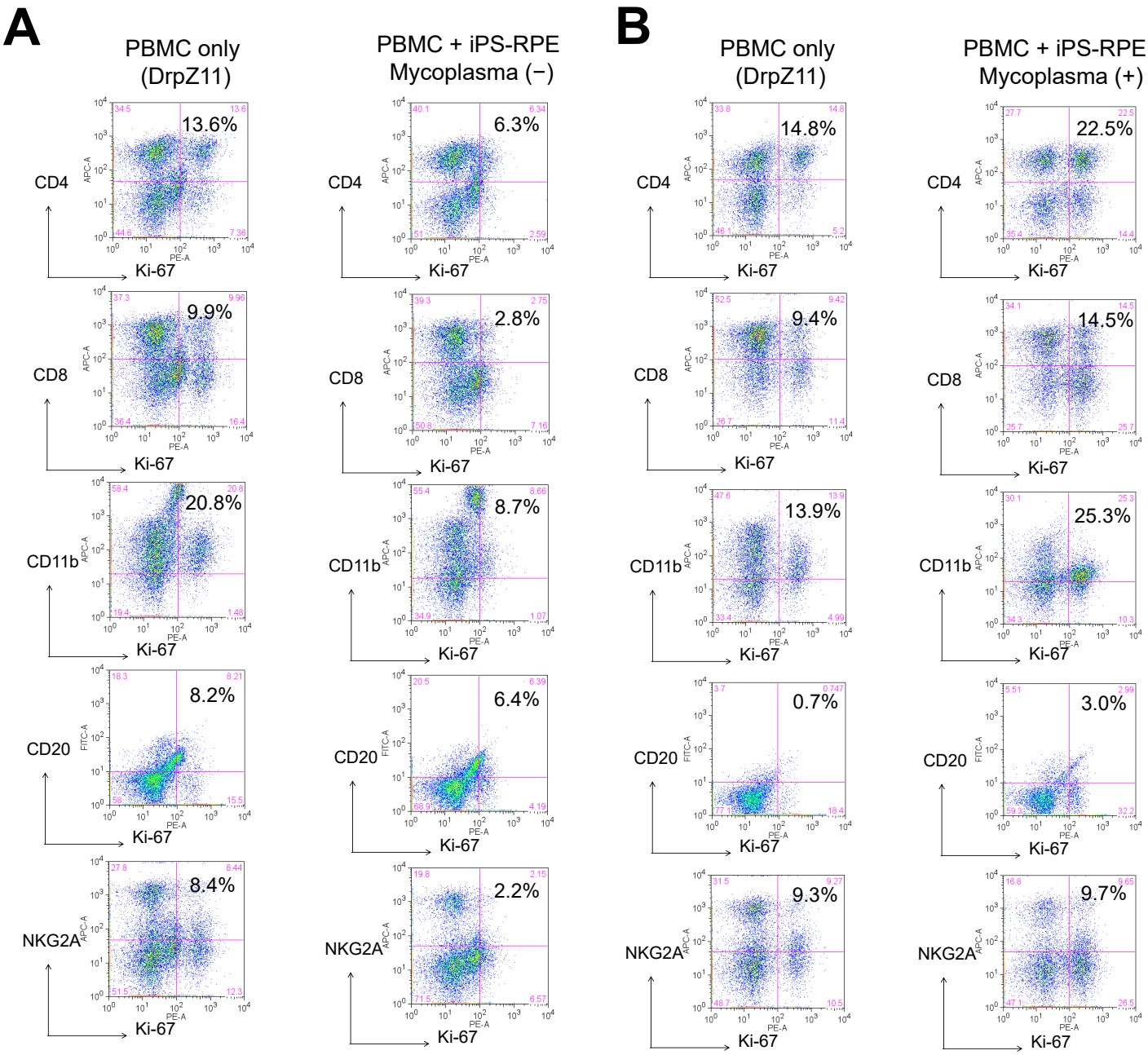
A
PBMC only
(DrpZ11)
PBMC + iPS-RPE
Mycoplasma (−)
CD4
13.6%
6.3%
CD8
9.9%
2.8%
CD11b
20.8%
8.7%
CD20
8.2%
6.4%
NKG2A
8.4%
2.2%
Ki-67
PE-A
APC-A
FITC-A
B
PBMC only
(DrpZ11)
PBMC + iPS-RPE
Mycoplasma (+)
14.8%
22.5%
9.4%
14.5%
13.9%
25.3%
0.7%
3.0%
9.3%
9.7%

Makabe et al.

Investigative Ophthalmology & Visual Science

Supplemental Information

Mycoplasma ocular infection in subretinal graft transplantation of iPS cells-derived retinal pigment epithelial cells

Kenichi Makabe, Sunao Sugita, Ayumi Hono, Hiroyuki Kamao, and Masayo Takahashi

Inventory of Supplemental Information

Supplemental Figure 1.

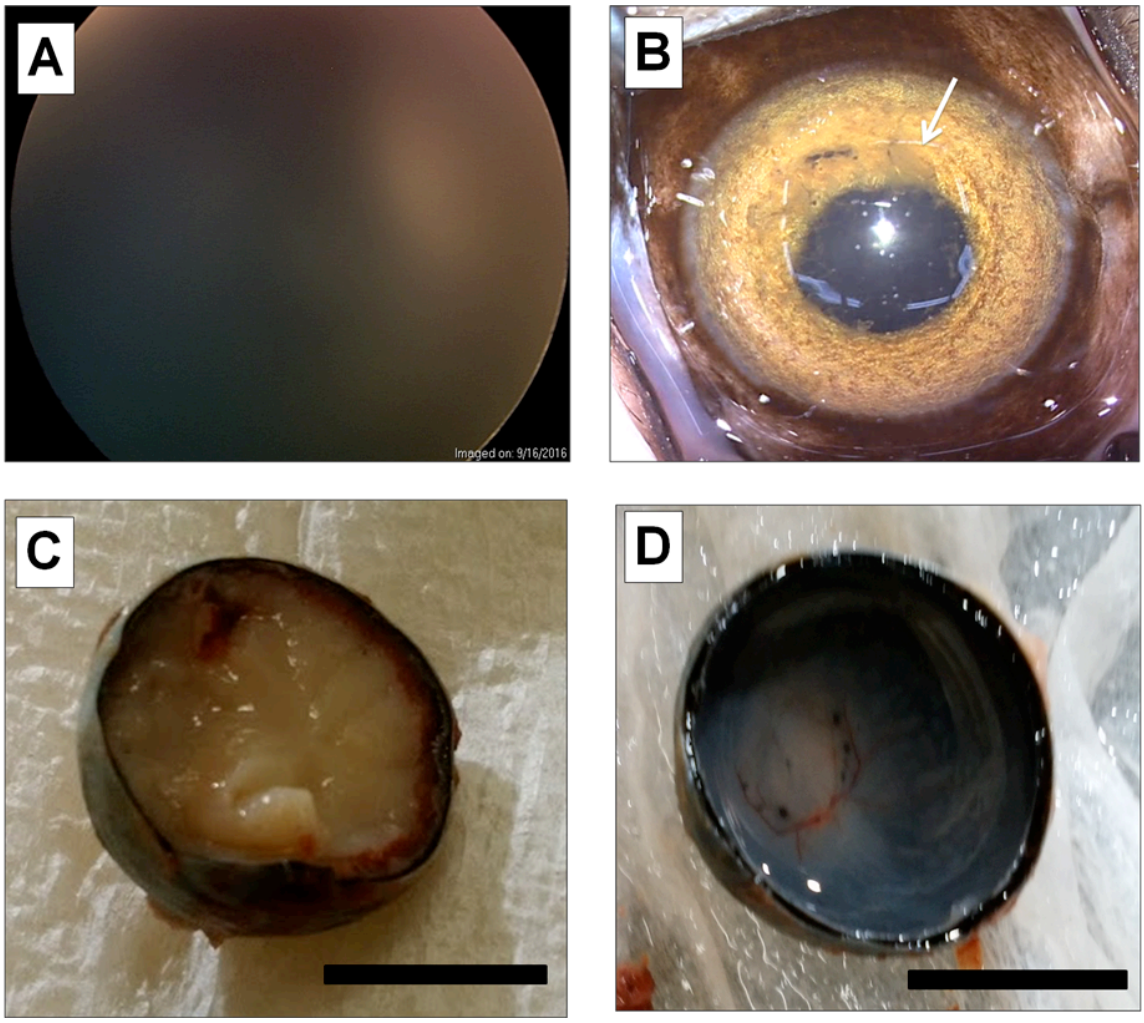

Inflammatory findings in the right eye of the DrpZ12 monkey.

(**A**) At 4 weeks after surgery, severe vitreous opacity was observed. (**B**) Iris rubeosis and fibrin (arrow) in the anterior chamber were seen in the anterior segment photos at 33 days after surgery. (**C**) Vitreous hemorrhage was found in the eyeball of the inflamed eye. (**D**) The retina and the vitreous are transparent in the control monkey eye that underwent iPS-RPE cell transplantation with a normal recovery course. Scale bar, 1 cm.

Supplemental Figure 2.

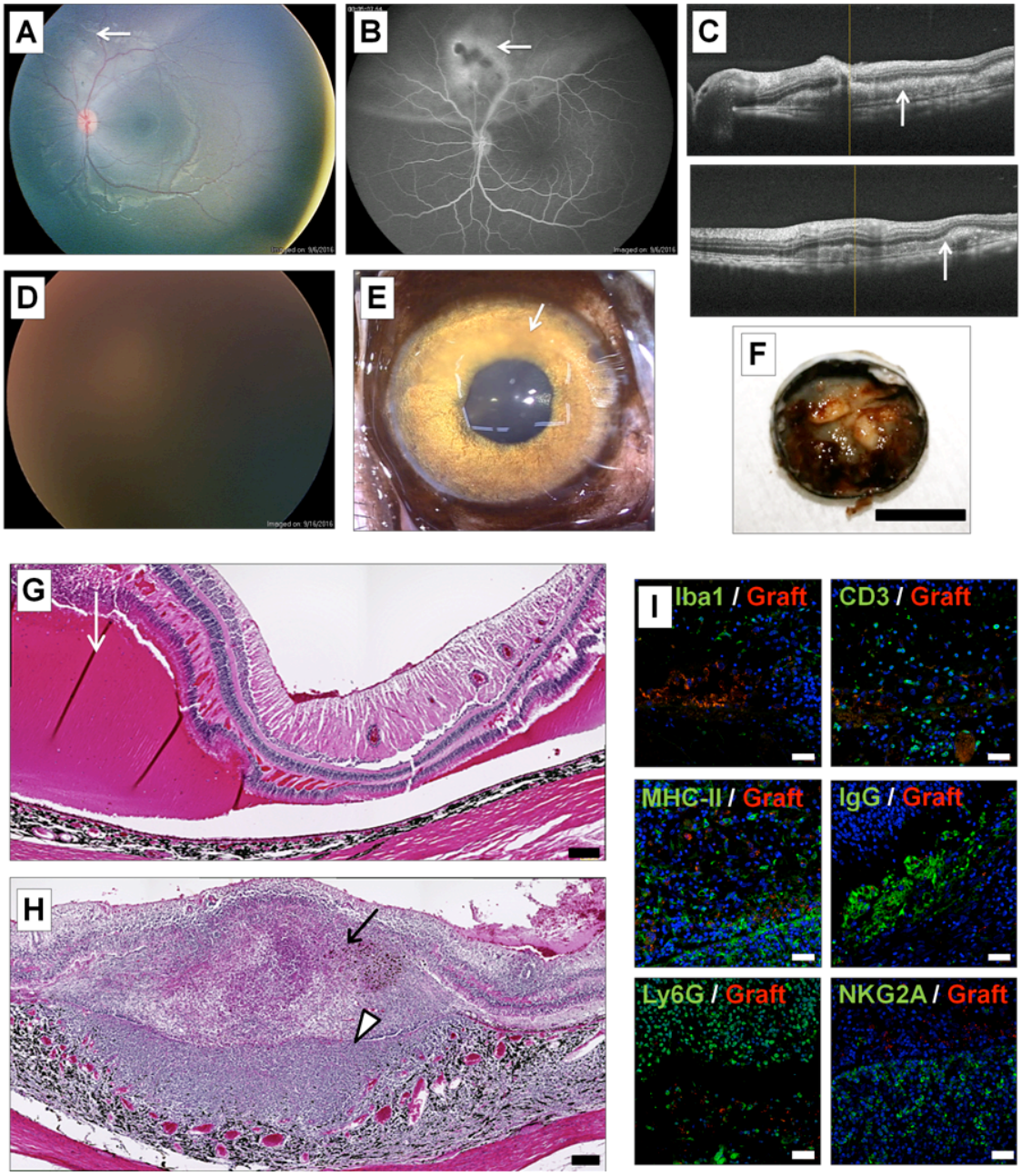

Inflammation after allogeneic transplantation in the left eye of the DrpZ12 monkey.
We explanted the monkey 1121A1 iPS-RPE cells (5 □ 10^5 cells with single-cell suspension) into the subretinal space in the left eye of the DrpZ12 MHC-matched monkey. (**A**) At 1 week after surgery, the fundus color photograph revealed no obvious abnormalities at the

implantation site (arrow). (**B**) Fluorescein angiography revealed leakage from the grafted cells (arrow). (**C**) In the OCT image, cell infiltration (arrow) was observed in the subretinal space of the implantation site. (**D**) Severe vitreous opacity was observed at 3 weeks after the surgery. (**E**) Iris rubeosis and fibrin (arrow) in the anterior chamber were seen in the anterior segment photos at 26 days after surgery. (**F**) Vitreous and retinal hemorrhages were seen in the eye. Scale bar, 1 cm. (**G**) Huge subretinal hemorrhages (arrow) were observed in the macula area. Scale bar, 200 μm. (**H**) Infiltration of inflammatory cells in the subretinal space (arrow) and thickened choroid were observed in the transplanted area (arrowhead). Scale bar, 200 μm. (**I**) In order to trace the cells after transplantation, we stained the graft iPS-RPE cells with PKH. Photomicrographs showing labeling of the DrpZ12 monkey retina in the left eye paraffin sections with anti-Iba1, MHC-II, CD3, Ly6G, NKG2A, and IgG antibodies. Large numbers of infiltrating $Iba1^+$ cells, $MHC\text{-}II^+$ cells, $CD3^+$ cells, $Ly6G^+$ cells, $NKG2A^+$ cells and IgG were observed around the PKH-positive iPS-RPE cell graft. Scale bar, 40 μm.

Supplemental Table 1. Results of MHC allele typing in the DrpZ11 and DrpZ12 monkeys.

MHC antigens	Name	DrpZ12		DrpZ11	
	Sex	Female		Female	
Mafa-Class I	Mafa-A1	A1*052:02	A1*094:01	A1*052:02	A1*094:01
	Mafa-A2–5	A4*01:02/04/11	A2*05:01/04/05	A4*01:02/04/11	A2*05:01/04/05
	Mafa-B	B*095:01 B*033:02 B*098:06	B*007:01:01/04 B*117:01/02 B*158:01 B*159:01 B*079:02	B*095:01 B*033:02	B*108:01 B*099:01 B*098:04 B*045:03like B*104:03
Mafa-Class II	Mafa-DRB sub-region	DRB1*03:21 DRB1*10:07	DRB*W4:01 DRB1*04:02:01	DRB1*03:21 DRB1*10:07	DRB1*03:07 DRB1*10:06
	Mafa-DQA1	DQA1*01:07:01	DQA1*01:08:04	DQA1*01:07:01	DQA1*01:20
	Mafa-DQB1	DQB1*06:08	DQB1*06:01:02	DQB1*06:08	DQB1*06:25
	Mafa-DPA1	DPA1*02:05	DPA1*04:02	DPA1*02:05	DPA1*07:02
	Mafa-DPB1	DPB1*15:04	DPB1*03:04	DPB1*15:04	DPB1*19:03